Inorg. Chem. **2008**, *47*, 7599−7607

4′-(5‴-R-Pyrimidyl)-2,2′:6′,2″-terpyridyl (R = H, OEt, Ph, Cl, CN) Platinum(II) Phenylacetylide Complexes: Synthesis and Photophysics

Zhiqiang Ji, Yunjing Li, and Wenfang Sun*

Department of Chemistry and Molecular Biology, North Dakota State University, Fargo, North Dakota 58105

Received February 25, 2008

A series of new square-planar 4′-(5‴-R-pyrimidyl)-2,2′:6′,2″-terpyridyl platinum(II) phenylacetylide complexes (**1a**−**5a**) bearing different substituents (R = H, OEt, Ph, Cl, CN) on the pyrimidyl ring have been synthesized and characterized. The electronic absorption, photoluminescence, and triplet transient difference absorption spectra were investigated. All of the complexes exhibit broad, moderately strong absorption between 400 and 500 nm that can be tentatively assigned to the metal-to-ligand charge transfer (^{1}MLCT) transition, possibly mixed with some ligand-to-ligand charge transfer (^{1}LLCT) character. Photoluminescence arising from the ^{3}MLCT state was observed both in fluid solutions at room temperature and in a rigid matrix at 77 K. The ^{1}MLCT/^{1}LLCT absorption bands and the ^{3}MLCT emission bands for **1a**−**5a** red-shift in comparison to those of the corresponding 4′-toly-2,2′:6′,2″-terpyridyl platinum(II) phenylacetylide complex. In addition, the energies of the ^{1}MLCT/^{1}LLCT absorption and the ^{3}MLCT emission bands exhibit a linear correlation with the Hammett constant (σ_p) of the 5‴-substituent on the pyrimidyl ring. The lifetime of the ^{3}MLCT emission at room temperature is governed by the energy gap law. The triplet transient difference absorption spectra of **1a**−**5a** exhibit a broad absorption band from 500 to 800 nm, and a bleaching band between 420 and 500 nm. Complex **5a**, which contains the −CN substituent, exhibits a lower-energy triplet absorption band at 785 nm and a shorter lifetime (130 ns) in CH_3CN than **2a**, which has the −OEt substituent, does (λ_{T1-Tn}^{max} = 720 nm, τ_T = 660 ns). The triplet excited-state absorption coefficients at the band maxima for **1a**−**5a** vary from 36 600 $L \cdot mol^{-1} \cdot cm^{-1}$ to 115 090 $L \cdot mol^{-1} \cdot cm^{-1}$, and the quantum yields of the triplet excited-state formation range from 0.19 to 0.66. All complexes exhibit a moderate nonlinear transmission for nanosecond laser pulses at 532 nm. Moreover, these complexes can generate singlet oxygen efficiently in air-saturated CH_3CN solutions, with the singlet oxygen generation quantum yield (Φ_Δ) varying from 0.24 to 0.46.

Introduction

Square-planar platinum terpyridyl (tpy) complexes[1] have attracted great interest in recent decades because of their unique spectroscopic properties and their potential applications in photonic devices and photosensitization, such as organic light-emitting devices,[2] photovoltaic cells,[3] chemical sensors,[4] photosensitized chemical reactions,[5] and so forth. Recently, our group discovered that some of the platinum(II) terpyridyl complexes could be promising nonlinear absorbing materials because of their broad and moderately strong excited-state absorption in the visible to the near-IR region.[1i,6] It has been reported that the substituent on the 4′ position of the terpyridyl ligand affects the photophysics of the platinum complexes drastically.[1c,g] Especially when a large aryl substituent, such as pyrenyl, was attached to the 4′ position

* Author to whom correspondence should be addressed. Phone: 701-231-6254. Fax: 701-231-8831. E-mail: Wenfang.Sun@ndsu.edu.

(1) (a) Aldridge, T. K.; Stacey, E. M.; McMillin, D. R. *Inorg. Chem.* **1994**, *33*, 722. (b) Buchner, R.; Field, J. S.; Haines, R. J.; Cunningham, C. T.; McMillin, D. R. *Inorg. Chem.* **1997**, *36*, 3952. (c) Crites, D. K.; Cunningham, C. T.; McMillin, D. R. *Inorg. Chim. Acta* **1998**, *273*, 346. (d) Buchner, R.; Cunningham, C. T.; Field, J. S.; Haines, R. J.; McMillin, D. R.; Summerton, G. C. *J. Chem. Soc., Dalton Trans.* **1999**, 711. (e) Lai, S.-W.; Chan, M. C. W.; Cheung, K.-K.; Che, C.-M. *Inorg. Chem.* **1999**, *38*, 4262. (f) Yam, V. W.-W.; Tang, R. P.-L.; Wong, K. M.-C.; Cheung, K.-K. *Organometallics* **2001**, *20*, 4476. (g) Micalec, J. F.; Ejune, S. A.; Cuttell, D. G.; Summerton, G. C.; Gertenbach, J. A.; Field, J. S.; Haines, R. J.; McMillin, D. R. *Inorg. Chem.* **2001**, *40*, 2193. (h) Yang, Q.-Z.; Wu, L.-Z.; Wu, Z.-X.; Zhang, L.-P.; Tung, C.-H. *Inorg. Chem.* **2002**, *41*, 5653. (i) Guo, F.; Sun, W.; Liu, Y.; Schanze, K. *Inorg. Chem.* **2005**, *44*, 4055. (j) Shikhova, E.; Danilov, E. O.; Kinayyigit, S.; Pomestchenko, I. E.; Tregubov, A. D.; Camerel, F.; Retailleau, P.; Ziessel, R.; Castellano, F. N. *Inorg. Chem.* **2007**, *46*, 3038. (k) Ziessel, R.; Diring, S. *Tetrahedron Lett.* **2006**, *47*, 4687. (l) Chen, W.-H.; Reinheimer, E. W.; Dunbar, K. R.; Omary, M. A. *Inorg. Chem.* **2006**, *45*, 2770.

10.1021/ic800358w CCC: $40.75
Published on Web 07/29/2008

of the terpyridyl ligand, the nature of the lowest excited state was altered.[1g] For a relatively small aryl substituent, such as phenyl, the effect was limited, partially due to the lack of coplanarity between the phenyl ring and the terpyridyl ligand. To improve the coplanarity, it is necessary to remove the repulsive interactions between the four hydrogens adjacent to the interannular bond. Hanan and co-workers reported that either replacing the 4′-phenyl substituent by a pyrimidyl ring or using a triazine ring to substitute the central pyridine ring could improve the coplanarity.[7] Ruthenium complexes using these approaches were synthesized and investigated.[7a–e,g] Coplanarity between the aryl substituent and the terpyridyl ligand (or the triazine-based terdentate ligand) was realized in these complexes, and the π conjugation was extended. Consequently, the metal-to-ligand charge transfer (MLCT) band in their UV−vis absorption spectra and the ^{3}MLCT-based emission band red-shifted. Most importantly, the emission lifetimes of the ruthenium complexes increased significantly. To verify whether these strategies are applicable to the d^8 transition-metal complexes and to explore how

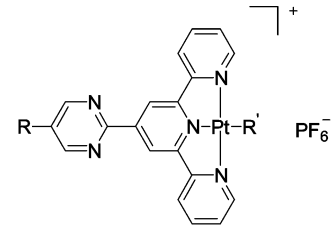

	R=	R'=		R=	R'=
1a	H		**1b**	H	
2a	OEt		**2b**	OEt	
3a	Ph	≡—	**3b**	Ph	Cl
4a	Cl		**4b**	Cl	
5a	CN		**5b**	CN	

Figure 1. Chemical structures of **1a**−**5a** and **1b**−**5b**.

significant the substituent on the pyrimidyl ring influences the photophysics of the d^8 transition-metal complexes, a series of 4′-(5‴-R-pyrimidyl)-2,2′:6′,2″-terpyridyl platinum(II) phenylacetylide complexes (**1a**−**5a**) bearing different substituents (R = H, OEt, Ph, Cl, CN; Figure 1) were synthesized and fully characterized by ^{1}H NMR, high resolution mass spectrometry (HRMS), and elemental analysis. Their electronic absorption, photoluminescence, and triplet excited-state characteristics were systematically investigated. The efficiency of these complexes to generate singlet oxygen was also evaluated. For comparison purposes, 4′-(5‴-R-pyrimidyl)-2,2′:6′,2″-terpyridyl platinum(II) chloride complexes (**1b**−**5b**) were also synthesized and studied. Additionally, the nonlinear transmission behavior of these complexes was investigated.

Experimental Section

Synthesis. 4′-CN-2,2′:6′,2″-Terpyridine,[8] 4′-(5‴-CN-pyrimidyl)-2,2′:6′,2″-terpyridine,[7e] 4′-(5‴-Cl-pyrimidyl)-2,2′:6′,2″-terpyridine,[7e] 4′-(5‴-Ph-pyrimidyl)-2,2′:6′,2″-terpyridine,[7e] 4′-pyrimidyl-2,2′:6′,2″-terpyridine,[7e] and 2-OEt-trimethinium perchlorate[9] were prepared according to the literature procedures. Silver phenylacetylide (AgC≡CPh) was synthesized by modification of the literature procedure.[10] All solvents were purchased from VWR Scientific Company at analytical grade and used without further purification unless otherwise stated. All reagents were purchased from Aldrich and Alfa Aesar and used as-is without further purification.

All products were characterized by ^{1}H NMR, HRMS, and elemental analysis. ^{1}H NMR spectra were obtained using a Varian 400 or 500 MHz VNMR spectrometer. All samples were analyzed by positive ion electrospray ionization (ESI) on a 12T Bruker APEX-Qe FTICR-MS with an Apollo II ion source at the Old Dominion University. Elemental analyses were conducted by NuMega Resonance laboratories, Inc. in San Diego, California.

4′-(5‴-OEt-Pyrimidyl)-2,2′:6′,2″-terpyridine. The synthesis is similar to that reported in the literature for other 4′-(5‴-R-

(2) (a) Lu, W.; Mi, B.-X.; Chan, M. C. W.; Hui, Z.; Che, C.-M.; Zhu, N.; Lee, S.-T. *J. Am. Chem. Soc.* **2004**, *126*, 4958. (b) Yersin, H.; Donges, D.; Humbs, W.; Strasser, J.; Sitters, R.; Glasbeek, M. *Inorg. Chem.* **2002**, *41*, 4915. (c) Brooks, J.; Babayan, Y.; Lamansky, S.; Djurovich, P. I.; Tsyba, I.; Bau, R.; Thompson, M. E. *Inorg. Chem.* **2002**, *41*, 3055. (d) Shi, J. C.; Chao, H. Y.; Fu, W. F.; Peng, S. M.; Che, C. M. *J. Chem. Soc., Dalton Trans.* **2000**, *18*, 3128. (e) Chassot, L.; von Zelewsky, A.; Sandrini, D.; Maestri, M.; Balzani, V. *J. Am. Chem. Soc.* **1986**, *108*, 6084. (f) Maestri, M.; Sandrini, D.; Balzani, V.; Chassot, L.; Jolliet, P.; von Zelewsky, A. *Chem. Phys. Lett.* **1985**, *122*, 375. (g) Wong, W.-Y.; He, Z.; So, S.-K.; Tong, K.-L.; Lin, Z. *Organometallics* **2005**, *24*, 4079.

(3) (a) Chakraborty, S.; Wadas, T. J.; Hester, H.; Flaschenreim, C.; Schmehl, R.; Eisenberg, R. *Inorg. Chem.* **2005**, *44*, 6284. (b) Chakraborty, S.; Wadas, T. J.; Hester, H.; Schmehl, R.; Eisenberg, R. *Inorg. Chem.* **2005**, *44*, 6865.

(4) (a) Yang, Q.-Z.; Wu, L.-Z.; Zhang, H.; Chen, B.; Wu, Z.-X.; Zhang, L.-P.; Tung, Z.-H. *Inorg. Chem.* **2004**, *43*, 5195. (b) Wu, L. Z.; Cheung, T. C.; Che, C. M.; Cheung, K. K.; Lam, M. H. W. *Chem. Commun.* **1998**, *10*, 1127. (c) Wong, K.-H.; Chan, M. C.-W.; Che, C. M. *Chem.—Eur. J.* **1999**, *5*, 2845. (d) Kui, S. C. F.; Chui, S. S.-Y.; Che, C.-M.; Zhu, N. *J. Am. Chem. Soc.* **2006**, *128*, 8297. (e) Wong, K. M.; Tang, W.-S.; Lu, X.-X.; Zhu, N.; Yam, V. W.-W. *Inorg. Chem.* **2005**, *44*, 1492. (f) Han, X.; Wu, L.-Z.; Si, G.; Pan, J.; Yang, Q.-Z.; Zhang, L.-P.; Tung, C.-H. *Chem.—Eur. J.* **2007**, *13*, 1231. (g) Wong, K. M.-C.; Tang, W.-S.; Chu, B. W.-K.; Zhu, N.; Yam, V. W.-W. *Organometallics* **2004**, *23*, 3459.

(5) (a) Zhang, D.; Wu, L.-Z.; Yang, Q.-Z.; Li, X.-H.; Zhang, L.-P.; Tung, C.-H. *Org. Lett.* **2003**, *5*, 3221. (b) Yang, Y.; Zhang, D.; Wu, L.-Z.; Chen, B.; Zhang, L.-P.; Tung, C.-H. *J. Org. Chem.* **2004**, *69*, 4788. (c) Li, X.-H.; Wu, L.-Z.; Zhang, L.-P.; Tung, C.-H.; Che, C. M. *Chem. Commun.* **2001**, *21*, 2280. (d) Feng, K.; Zhang, R.-Y.; Wu, L.-Z.; Tu, B.; Peng, M.-L.; Zhang, L.-P.; Zhao, D.; Tung, C.-H. *J. Am. Chem. Soc.* **2006**, *128*, 14685.

(6) (a) Sun, W.; Wu, Z.-X.; Yang, Q.-Z.; Wu, L.-Z.; Tung, C.-H. *Appl. Phys. Lett.* **2003**, *82*, 850. (b) Sun, W.; Guo, F. *Chin. Opt. Lett.* **2005**, *S3*, S34. (c) Guo, F.; Sun, W. *J. Phys. Chem. B* **2006**, *110* (30), 15029. (d) Pritchett, T. M.; Sun, W.; Guo, F.; Zhang, B.; Ferry, M. J.; Rogers-Haley, J. E.; Shensky, W.; Mott, A. G. *Opt. Lett.* **2008**, *33* (10), 1053.

(7) (a) Passalacqua, R.; Loiseau, F.; Campaigns, S.; Fang, Y.; Hanan, G. S. *Angew. Chem., Int. Ed.* **2003**, *42*, 1608. (b) Polson, M. I. J.; Taylor, N. J.; Hanan, G. S. *Chem. Commun.* **2002**, 1356. (c) Polson, M. I. J.; Medlycott, E. A.; Hanan, G. S.; Mikelsons, L.; Taylor, N. J.; Watanabe, M.; Tanaka, Y.; Loiseau, F.; Passalacqua, R.; Campagna, S. *Chem.—Eur. J.* **2004**, *10*, 3640. (d) Medlycott, E. A.; Hanan, G. S. *Chem. Commun.* **2007**, 4884. (e) Fang, Y.-Q.; Taylor, N. J.; Laverdiere, F.; Hanan, G. S.; Loiseau, F.; Nastasi, F.; Campagna, S.; Nierengarten, H.; Leize-Wagner, E.; Dorsselaer, A. V. *Inorg. Chem.* **2007**, *46*, 2854. (f) Medlycott, E. A.; Hanan, G. S. *Coord. Chem. Rev.* **2006**, *250*, 1763. (g) Fang, Y.-Q.; Taylor, N. J.; Hanan, G. S.; Loiseau, F.; Passalacqua, R.; Campagna, S.; Nierengarten, H.; Dorsselaer, A. V. *J. Am. Chem. Soc.* **2002**, *124*, 7912.

(8) Veauthier, J. M.; Carlson, C. N.; Collis, G. E.; Kiplinger, J. K.; John, K. D. *Synthesis* **2005**, 2683.

(9) Wagner, E. R.; Matthews, D. P.; Barney, C. L. U.S. patent 4788335, 1988.

(10) Agawa, T.; Miller, S. I. *J. Am. Chem. Soc.* **1961**, *83*, 449.

pyrimidyl)-2,2′:6′,2″-terpyridine.[7e] Yield: 54%. ^{1}H NMR ($CDCl_3$, 500 MHz): δ 1.54 (3H, t, J = 6.5 Hz), 4.26 (2H, q, J = 7.0 Hz), 7.37 (2H, dt, J = 1.0, 5.5 Hz), 7.90 (2H, dt, J = 1.5, 7.5 Hz), 8.58 (2H, s), 8.68 (2H, d, J = 7.5 Hz), 8.79 (2H, d, J = 3.5 Hz), 9.41 (2H, s).

General Procedure for the Synthesis of [(5-R-*Pm*-tpy)Pt-Cl]PF_6. A total of 1 mmol of 5-R-*Pm*-tpy ligand and 1 mmol of $Pt(DMSO)_2Cl_2$ was dissolved in 30 mL of $CHCl_3$, and the mixture was refluxed for 24 h. After that, the reaction mixture was concentrated and cooled down to room temperature. The solid was then filtered out and dissolved in a small amount of N,N-dimethylformamide (DMF). Saturated NH_4PF_6 aqueous solution was added, and the mixture was stirred at room temperature for 3 h. The resultant solid was filtered out; washed with water, methanol, and ether; and dried. The pure product was obtained by recrystalization in DMF/Et_2O.

[(5-H-*Pm*-tpy)PtCl]PF_6 (1b). Yield: 70%. ^{1}H NMR (d_6-DMSO, 400 MHz): δ 7.79 (1H, t, J = 4.8 Hz), 7.99 (2H, t, J = 6.0 Hz), 8.50 (2H, dt, J = 1.6, 8.0 Hz), 8.93 (2H, d, J = 8.0 Hz), 9.00 (2H, d, J = 5.2 Hz), 9.15 (2H, d, J = 4.8 Hz), 9.34 (2H, s). ESI-MS m/z calcd for $[C_{19}H_{13}ClN_5Pt^{194}]^+$: 540.0486. Found: 540.0468 (99%). ESI-MS m/z calcd for $[C_{19}H_{13}ClN_5Pt^{195}]^+$: 541.0507. Found: 541.0490 (100%). ESI-MS m/z calcd for $[C_{19}H_{13}ClN_5Pt^{196}]^+$: 542.0509. Found: 542.0492 (72%). Anal. calcd for $C_{19}H_{13}ClF_6N_5PPt.0.5CHCl_3$: C, 31.37; H, 1.82; N, 9.38. Found: C, 31.64; H, 1.73; N, 9.53.

[(5-Ph-*Pm*-tpy)PtCl]PF_6 (3b). Yield: 75%. ^{1}H NMR (CD_3CN, 400 MHz): δ 7.63 (3H, m), 7.88 (4H, m), 8.39 (2H, dt, J = 1.6, 8.0 Hz), 8.50 (2H, m), 9.05 (2H, m), 9.21 (2H, s), 9.32 (2H, s). ESI-MS m/z calcd for $[C_{25}H_{17}ClN_5Pt^{194}]^+$: 616.0799. Found: 616.0770 (68%). ESI-MS m/z calcd for $[C_{25}H_{17}ClN_5Pt^{195}]^+$: 617.0820. Found: 617.0790 (100%). ESI-MS m/z calcd for $[C_{25}H_{17}ClN_5Pt^{196}]^+$: 618.0822. Found: 618.0794 (65%). Anal. calcd for $C_{25}H_{17}ClF_6N_5PPt$: C, 39.36; H, 2.25; N, 9.18. Found: C, 39.03; H, 2.62; N, 9.51.

[(5-Cl-*Pm*-tpy)PtCl]PF_6 (4b). Yield: 65%. ^{1}H NMR (CD_3CN, 500 MHz): δ 7.91 (2H, t, J = 5.0 Hz), 8.41 (2H, t, J = 4.0 Hz), 8.51 (2H, m), 9.08 (2H, m), 9.12 (2H, s), 9.18 (2H, s). ESI-MS m/z calcd for $[C_{19}H_{12}Cl_2N_5Pt^{194}]^+$: 574.0096. Found: 574.0074 (85%). ESI-MS m/z calcd for $[C_{19}H_{12}Cl_2N_5Pt^{195}]^+$: 575.0117. Found: 575.0097 (100%). ESI-MS m/z calcd for $[C_{19}H_{12}Cl_2N_5Pt^{196}]^+$: 576.0119. Found: 576.0096 (69%). Anal. calcd for $C_{19}H_{12}Cl_2F_6N_5PPt$: C, 31.64; H, 1.68; N, 9.71. Found: C, 31.40; H, 1.77; N, 9.73.

[(5-CN-*Pm*-tpy)PtCl]PF_6 (5b). Yield: 59%. ^{1}H NMR (CD_3CN, 400 MHz): δ 7.86 (2H, dt, J = 1.2, 5.6 Hz), 8.41 (2H, dt, J = 1.2, 8.0 Hz), 8.48 (2H, m), 9.02 (2H, m), 9.19 (2H, s), 9.37 (2H, s). ESI-MS m/z calcd for $[C_{20}H_{12}ClN_6Pt^{194}]^+$: 565.0439. Found: 565.0417 (83%). ESI-MS m/z calcd for $[C_{20}H_{12}ClN_6Pt^{195}]^+$: 566.0460. Found: 566.0440 (100%). ESI-MS m/z calcd for $[C_{20}H_{12}ClN_6Pt^{196}]^+$: 567.0461. Found: 567.0440 (66%). Anal. calcd for $C_{20}H_{12}ClF_6N_6PPt$: C, 33.75; H, 1.70; N, 11.81. Found: C, 33.38; H, 2.02; N, 11.88.

General Procedure for the Synthesis of [(5-R-*Pm*-tpy)Pt(C≡CC_6H_5)]PF_6. A total of 1 mmol of [(5-R-*Pm*-tpy)Pt-Cl]PF_6 was dissolved in 5 mL of DMF, and 1 mmol of corresponding silver salt was dissolved in 5 mL of pyridine. The two solutions were mixed together, and the resultant mixture was stirred under Ar for 24 h. Pyridine was removed, and an excess amount of ether was added. The solid was separated by centrifuge. The crude product was then purified by column chromatography using neutral Al_2O_3. The column was first flushed by CH_2Cl_2, and then CH_3CN was used as the eluent. The red layer was collected as the product. After removal of the solvent, the solid was recrystalized in CH_3CN/Et_2O.

[(5-H-*Pm*-tpy)Pt(C≡CC_6H_5)]PF_6 (1a). Yield: 74%. ^{1}H NMR (CD_3CN, 500 MHz): δ 7.13 (3H, m), 7.25 (1H, d, J = 7.5 Hz), 7.53 (2H, dt, J = 5.5, 1.5 Hz), 7.62 (2H, t, J = 5.0 Hz), 8.25 (4H, m), 8.74 (2H, m), 8.99 (2H, d, J = 12.5 Hz), 9.02 (2H, s). ESI-MS m/z calcd for $[C_{27}H_{18}N_5Pt^{194}]^+$: 606.1189. Found: 606.1183 (73%). ESI-MS m/z calcd for $[C_{27}H_{18}N_5Pt^{195}]^+$: 607.1210. Found: 607.1196 (100%). ESI-MS m/z calcd for $[C_{27}H_{18}N_5Pt^{196}]^+$: 608.1211. Found: 608.1209 (85%). Anal. calcd for $C_{27}H_{18}F_6N_5PPt$: C, 43.09; H, 2.41; N, 9.31. Found: C, 42.74; H, 2.54; N, 9.65.

[(5-OEt-*Pm*-tpy)Pt(C≡CC_6H_5)]PF_6 (2a). Yield: 35%. ^{1}H NMR (d_6-DMSO, 500 MHz): δ 1.48 (3H, t, J = 7.0 Hz), 4.39 (2H, q, J = 7.0 Hz), 7.27 (3H, m, J = 7.0, 7.5 Hz), 7.40 (2H, dt), 7.85 (2H, m), 8.41 (2H, m), 8.78 (4H, m), 9.00 (2H, m), 9.20 (2H, m). ESI-MS m/z calcd for $[C_{29}H_{22}N_5OPt^{194}]^+$: 650.1451. Found: 650.1432 (71%). ESI-MS m/z calcd for $[C_{29}H_{22}N_5OPt^{195}]^+$: 651.1472. Found: 651.1454 (100%). ESI-MS m/z calcd for $[C_{29}H_{22}N_5OPt^{196}]^+$: 652.1474. Found: 652.1452 (85%). Anal. calcd for $C_{29}H_{22}F_6N_5OPPt$: C, 43.73; H, 2.78; N, 8.79. Found: C, 43.55; H, 2.78; N, 8.79.

[(5-Ph-*Pm*-tpy)Pt(C≡CC_6H_5)]PF_6 (3a). Yield: 32%. ^{1}H NMR (d_6-DMSO, 500 MHz): δ 7.24 (3H, m), 7.48 (2H, m), 7.65 (3H, m), 7.93 (2H, m), 8.02 (2H, d, J = 7.5 Hz), 8.49 (2H, m), 8.93 (2H, m), 9.13 (2H, m), 9.45 (2H, m). ESI-MS m/z calcd for $[C_{33}H_{22}N_5Pt^{194}]^+$: 682.1502. Found: 682.1457 (36%). ESI-MS m/z calcd for $[C_{33}H_{22}N_5Pt^{195}]^+$: 683.1523. Found: 683.1489 (100%). ESI-MS m/z calcd for $[C_{33}H_{22}N_5Pt^{196}]^+$: 684.1524. Found: 684.1499 (72%). Anal. calcd for $C_{33}H_{22}F_6N_5PPt\cdot CH_2Cl_2$: C, 44.70; H, 2.65; N, 7.67. Found: C, 45.02; H, 2.53; N, 8.10.

[(5-Cl-*Pm*-tpy)Pt(C≡CC_6H_5)]PF_6 (4a). Yield: 63%. ^{1}H NMR (d_6-DMSO, 500 MHz): δ 7.33 (3H, m), 7.35 (2H, m), 7.95 (2H, m), 8.52 (2H, m), 8.86 (2H, m), 9.17 (2H, m), 9.30 (2H, m), 9.37 (2H, m). ESI-MS m/z calcd for $[C_{27}H_{17}ClN_5Pt^{194}]^+$: 640.0799. Found: 640.0766 (58%). ESI-MS m/z calcd for $[C_{27}H_{17}ClN_5Pt^{195}]^+$: 641.0820. Found: 641.0789 (100%). ESI-MS m/z calcd for $[C_{27}H_{17}ClN_5Pt^{196}]^+$: 642.0822. Found: 642.0787 (81%). Anal. calcd for $C_{27}H_{17}ClF_6N_5PPt$: C, 41.21; H, 2.18; N, 8.90. Found: C, 41.60; H, 2.03; N, 9.29.

[(5-CN-*Pm*-tpy)Pt(C≡CC_6H_5)]PF_6 (5a). Yield: 80%. ^{1}H NMR (d_6-DMSO, 500 MHz): δ 6.90 (5H, m), 7.39 (2H, m), 8.10 (2H, m), 8.25 (2H, m), 8.47 (2H, m), 8.91 (2H, m), 8.30 (2H, m). ESI-MS m/z calcd for $[C_{28}H_{17}N_6Pt^{194}]^+$: 631.1141. Found: 631.1117 (86%). ESI-MS m/z calcd for $[C_{28}H_{17}N_6Pt^{195}]^+$: 632.1162. Found: 632.1141 (100%). ESI-MS m/z calcd for $[C_{28}H_{17}N_6Pt^{196}]^+$: 633.1164. Found: 633.1140 (61%). Anal. calcd for $C_{28}H_{17}F_6N_6PPt\cdot H_2O$: C, 42.27; H, 2.41; N, 10.56. Found: C, 41.87; H, 2.21; N, 10.74.

Photophysical Studies. The electronic absorption spectra were recorded on a SHIMADZU 2501 PC UV−vis spectrophotometer. Complexes **1a**−**5a**, **1b**, and **3b**−**5b** were dissolved in CH_3CN. The emission spectra at room temperature, 77 K, and in the solid state were all recorded on a SPEX Fluorolog-3 fluorometer/phosphorometer. The complexes were dissolved in CH_3CN for room temperature measurement. The low-temperature (77 K) emission was measured in butyronitrile (BuCN) glassy solutions. The solutions were degassed for 30 min prior to each measurement. The solid-state emission was measured using a quartz slide with thin films of complexes **1a**−**5a** formed on it through solvent evaporation. The slide was placed 45° to the excitation beam. The emission lifetimes were measured on an Edinburgh LP920 laser flash photolysis spectrometer. Excitation was provided by the third-harmonic output (355 nm) of a Quantel Brilliant Q-switched Nd:YAG laser (fwhm pulsewidth was 4.1 ns and the repetition rate set at 1 Hz). Sample solutions were degassed for 30 min before each

measurement. The emission quantum yields of the complexes were determined by the comparative method,[11] in which a degassed aqueous solution of $[Ru(bpy)_3]Cl_2$ ($\phi_{em} = 0.042$, excited at 436 nm)[12] was used as the reference.

The triplet transient difference absorption spectra were measured on an Edinburgh LP920 laser flash photolysis spectrometer. Excitation was provided by the third-harmonic output (355 nm) of the Quantel Brilliant Q-switched Nd:YAG laser. The solutions were degassed with Ar for 30 min before each measurement. The absorbance of the solution was adjusted to $A = 0.4$ at 355 nm in a 1 cm quartz cuvette. The triplet excited-state absorption coefficient (ε_T) at the absorption band maximum was measured by the singlet depletion method[13] (see the Supporting Information for details). The quantum yields of the triplet excited-state formation (Φ_T) were determined using the comparative method[14] (see the Supporting Information for details). SiNc in benzene ($\Phi_T = 0.20$, $\varepsilon = 70\,000$ $M^{-1}cm^{-1}$)[15] was used as the reference.

The singlet oxygen generation quantum yields were evaluated by the comparative method[16] using an Edinburgh TL900 transient luminescence spectrometer. The third-harmonic output (355 nm) of the Quantel Nd:YAG laser was used as the excitation source. An ultrasensitive, ultrafast germanium detector EI-P was used to monitor the emission of the singlet oxygen at 1270 nm. A silicon cutoff filter (>1100 nm) was used to eliminate the scattered light from the laser. The experimental details are provided in the Supporting Information.

The nonlinear transmission experimental setup and details have been described previously.[17]

Results and Discussion

Electronic Absorption. Figure 2 displays the electronic absorption spectra of **1a**−**5a**, **1b**, and **3b**−**5b**. The absorption band maxima and extinction coefficients are listed in Table 1. In the concentration range of 5×10^{-6} M to 1×10^{-4} M in CH_3CN solution, the absorption of **1a**−**5a** obeys Beer−Lambert's law, indicating that no ground-state aggregation occurs in this concentration range. All complexes exhibit intensive absorption between 250 and 350 nm, which is ascribed to the intraligand $^1\pi,\pi^*$ transitions. Complexes **2a**, **3a**, and **3b** with an electron-donating substituent, that is, −OEt and −Ph, on the pyrimidyl moiety exhibit a slightly hypsochromic shift in the bands below 300 nm, but an increased intensity in the band between 300 and 350 nm in comparison to the complexes with an electron-withdrawing substituent, that is, −Cl and −CN, and the one without a substituent on the pyrimidyl moiety. The broad band between 400 and 500 nm for **1a**−**5a** and at ca. 410 nm for **1b** and **3b**−**5b** are in line with the $d\pi(Pt) \rightarrow \pi^*$(terpyridyl)/$\pi$(C≡CR) → π^*(terpyridyl) transitions in the reported 4′-tolylterpyridyl platinum(II) complexes[1f,h,i] with respect to energy and the extinction coefficient. A time-dependent density functional theory calculation by Feng and co-workers on 4′-tolylterpyridyl platinum(II) acetylide complexes also revealed that the highest occupied molecular orbital (HOMO) has a predominant contribution from the acetylide moiety and some contribution from the Pt d orbital, while the lowest unoccupied molecular orbital (LUMO) is dominated by the terpyridyl ligand.[18] Therefore, the lower-energy absorption band of **1a**−**5a**, **1b**, and **3b**−**5b** is tentatively assigned to the spin-allowed ^{1}MLCT, possibly mixed with some ligand-to-ligand charge transfer (^{1}LLCT) character. However, due to the stronger electron-donating ability of the phenylacetylide ligand in **1a**−**5a**, the $d\pi(Pt)/\pi(C{\equiv}CR)$-based HOMO is destabilized while the terpyridyl-based LUMO is almost unaffected. As a result, the energy gap between the HOMO and the LUMO decreases, resulting in a pronounced broadening and bathochromic shift in their ^{1}MLCT/^{1}LLCT bands in contrast to their corresponding chloride complexes (**1b**, **3b**−**5b**).

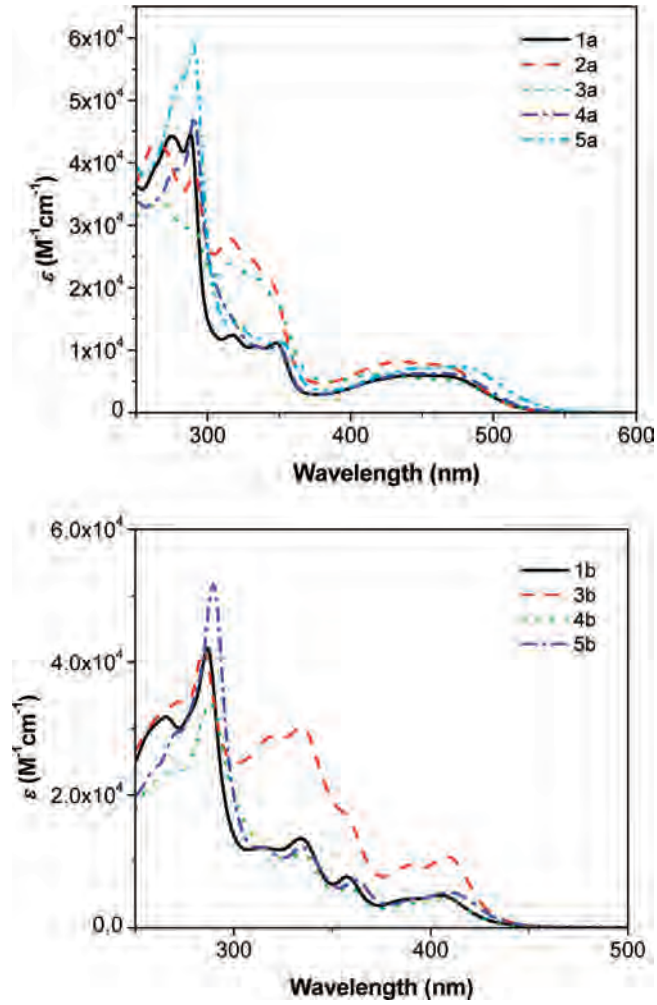

Figure 2. UV−vis spectra of **1a**−**5a**, **1b**, and **3b**−**5b** in CH_3CN solutions.

(11) Demas, J. N.; Crosby, G. A. *J. Phys. Chem.* **1971**, *75*, 991.
(12) Van Houten, J.; Watts, R. J. *J. Am. Chem. Soc.* **1976**, *98*, 4853.
(13) Carmichael, I.; Hug, G. L. *J. Phys. Chem. Ref. Data* **1986**, *15*, 1.
(14) (a) Bensasson, R.; Goldschmidt, C. R.; Land, E. J.; Truscott, T. G. *Photochem. Photobiol.* **1978**, *28*, 277. (b) Foley, S.; Jones, G.; Liuzzi, R.; McGarvey, D. J.; Perry, M. H.; Truscott, T. G. *J. Chem. Soc., Perkin Trans. 2* **1997**, *2*, 1725. (c) Kumar, C. V.; Qin, L.; Das, P. K. *J. Chem. Soc., Faraday Trans.* **1984**, *280*, 783.
(15) Firey, P. A.; Ford, W. E.; Sounik, J. R.; Keney, M. E.; Rodgers, M. A. J. *J. Am. Chem. Soc.* **1988**, *110*, 7626.
(16) Abdel-Shafi, A. A.; Beer, P. D.; Mortimer, R. J.; Wilkinson, F. *Phys. Chem. Chem. Phys.* **2000**, *2*, 3137.
(17) (a) Sun, W.; Dai, Q.; Worden, J. G.; Huo, Q. *J. Phys. Chem. B* **2005**, *109*, 20854. (b) Li, Y.; Dini, D.; Calvete, M. J. F.; Hanack, M.; Sun, W. *J. Phys. Chem. A* **2008**, *112* (3), 472.
(18) Liu, X.-J.; Feng, J.-K.; Meng, J.; Pan, Q.-J.; Ren, A.-M.; Zhou, X.; Zhang, H.-X. *Eur. J. Inorg. Chem.* **2005**, 1856.

Table 1. Photophysical Data for **1a**−**5a**, **1b**, and **3b**−**5b**

	λ_{abs}/nm (ε/L·mol^{-1}·cm^{-1})[a]	λ_{em}/nm (τ /ns; Φ_{em}),[b] R.T.	k_r[c]/10^4 s^{-1}, R.T.	k_{nr}[d]/10^6 s^{-1}, R.T.	λ_{em}/nm (τ /μs),[e] 77K	λ_{em}/nm solid, R.T.
1a	275 (44220), 288 (44540) 317 (12420), 334 (10620) 348 (11180), 441 (5980), 469 (5820)	618 (380; 0.0039)	1.0	2.6	570 (11.9), 630 (3.4)	665
2a	263 (43560), 291 (38240) 315 (27880), 432 (8140) 460 (7720)	612 (700; 0.0058)	0.8	1.4	572 (10.0), 624 (3.4)	674
3a	263 (33320), 272 (33000) 289 (29840), 318 (23940) 413 (6140), 466 (5300)	618 (400; 0.0040)	1.0	2.5	520 (12.6), 576 (11.1), 619 (6.3)	691
4a	291 (47400), 349 (10780) 443 (6240), 474 (6270)	621 (340; 0.0032)	0.9	2.9	528 (12.8), 570 (12.5), 628 (5.1)	612
5a	291 (58960), 319 (14340) 351 (11320), 453 (7180) 476 (7320)	639 (130; 0.0011)	0.8	7.7	599 (8.8), 662 (2.8)	668
1b	266 (31710), 287 (42070) 334 (13460), 357 (7680) 387 (4270), 404 (4960)				502 (17.7), 539 (17.1), 577 (7.2)	
3b	272 (33970), 285 (42010) 320 (28910), 334 (30230) 390 (9370), 408 (10800)				523 (8.8, 12%; 34.0, 88%), 577 (4.8, 23%; 30.0, 77%), 608 (4.7), 620 (4.5)	
4b	270 (23740), 288 (34040) 334 (11290), 358 (6130) 389 (3670), 406 (4340)				505 (19.5), 543 (19.0), 589 (5.0)	
5b	290 (51700), 335 (12050) 362 (7190), 409 (5360)				510 (20.4), 551 (19.1), 600 (4.7)	

[a] Electronic absorption band maxima and molar extinction coefficients in CH_3CN solutions. [b] Room temperature emission band maxima and decay lifetimes measured at a concentration of 5×10^{-5} mol/L, and emission quantum yields measured at solutions with $A_{436} = 0.1$ in CH_3CN solutions. [c] Radiative decay rate $k_r = \Phi_{em}/\tau$. [d] Nonradiative decay rate $k_{nr} = (1 - \Phi_{em})/\tau$. [e] Emission band maxima and decay lifetimes in butyronitrile glassy solutions; the concentration of the solutions is 1×10^{-4} mol/L.

The substituent at the 5‴ position of the pyrimidyl ring exhibits a pronounced effect on the energy of the ^{1}MLCT/^{1}LLCT band. A linear correlation between the lowest energy of the ^{1}MLCT/^{1}LLCT band and the Hammett constant (σ_p) of the substituent was observed in **1a**−**5a** (see Figure S1 in the Supporting Information). This is not surprising because the coplanarity of the pyrimidyl ring with the terpyridyl ligand would allow for conjugation with the terpyridyl ligand to occur. The inductive and resonant effects from the 5‴ substituent would then influence the energy of the terpyridyl-based LUMO, which in turn causes the change of the lowest excited-state energy.

The ^{1}MLCT/^{1}LLCT bands are sensitive to solvent polarity. Lower-polarity solvents, such as CH_2Cl_2, cause a bathochromic shift of the ^{1}MLCT/^{1}LLCT band in comparison to that in CH_3CN. For example, the ^{1}MLCT/^{1}LLCT band of **2a** in CH_2Cl_2 appears at 482 nm, but in CH_3CN, it is at 437 nm. The red-shift of the ^{1}MLCT/^{1}LLCT band in low-polarity solvents compared to that in high-polarity solvents indicates that the ground states of these complexes are more polar than the excited states, which is consistent with the charge-transfer nature of the excited state.

Photoluminescence. Complexes **1a**−**5a** emit both at room temperature in acetonitrile solutions and in a butyronitrile rigid matrix at 77 K. At room temperature, the emission appears between 610 and 640 nm (Figure 3 and Table 1), which is more than a 150 nm Stokes shift with respect to the excitation spectra (see Supporting Information Figure S2). This feature along with the relatively long lifetime (hundreds of nanoseconds) suggests that the emission originates from a triplet excited state. With reference to the emission of other platinum terpyridyl complexes,[1–9] the emitting state is tentatively assigned to the ^{3}MLCT state. The emission

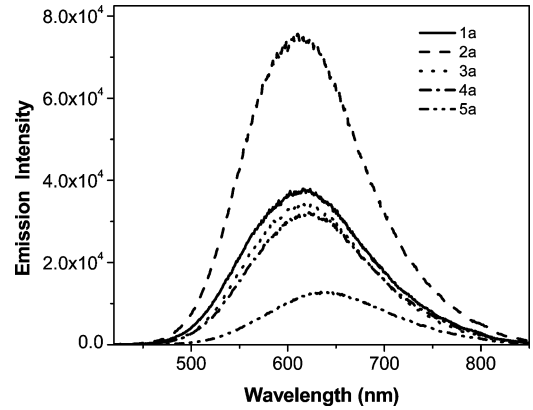

Figure 3. Room temperature emission spectra of **1a**−**5a** in CH_3CN solutions. The solution concentration was 5×10^{-5} M. The excitation wavelength was 355 nm.

energies of these complexes exhibit a linear correlation with the Hammett σ_p constant (see Supporting Information Figure S3), reflecting the electronic delocalization ability of the pyrimidyl group.[7e] The emission lifetime and the emission quantum yield (listed in Table 1) increase with increased emission energy. For example, **5a**, which emits at ca. 640 nm, possesses the shortest lifetime (130 ns) and the lowest emission quantum yield (0.11%), while **2a**, with $\lambda_{em} = 612$ nm, exhibits the longest lifetime (700 ns) and the highest quantum yield (0.58%). These phenomena are consistent with the energy gap law,[19] which describes the exponential increase of the nonradiative decay rate with decreased emission energy. As evident in Figure 4, a linear relationship with a negative slope is obtained on plotting ln k_{nr} versus E_{em}^{max} for **1a**−**5a**.

(19) Caspar, J. V.; Meyer, T. J. *J. Phys. Chem.* **1983**, *87*, 952.

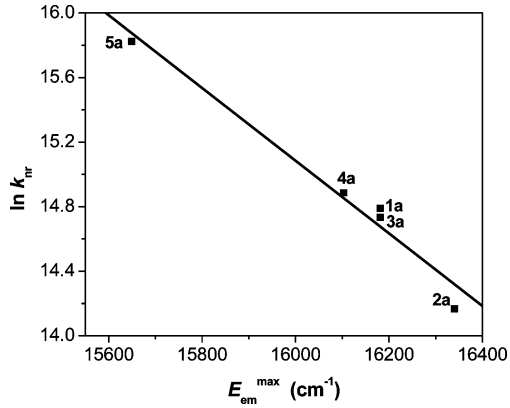

Figure 4. Plot of ln k_{nr} vs E_{em}^{max} for **1a**−**5a**.

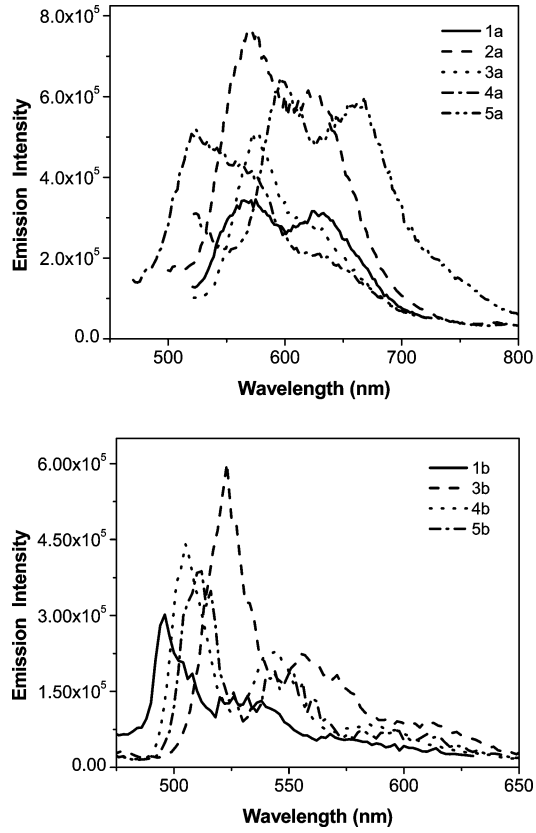

Figure 5. The 77 K emission spectra of **1a**−**5a**, **1b**, and **3b**−**5b** in BuCN glassy solutions. The solution concentration was 1×10^{-4} M, and the excitation wavelength was the ^{1}MLCT band maximum.

In contrast to **1a**−**5a**, no room temperature emission was observed in **1b** and **3b**−**5b**. The lack of emission of the platinum terpyridyl chloride complexes is common due to the presence of a thermally accessible low-lying, nonemissive metal-centered (MC) excited state,[1h] which adds an additional decay path for the ^{3}MLCT state. When the phenylacetylide ligand replaces the chloride ligand, the stronger π-donating ability of the phenylacetylide ligand increases the platinum-based HOMO, while the terpyridyl-based LUMO is essentially unaffected. Consequently, the energy gap between the HOMO and the LUMO decreases, resulting in a larger separation of the ^{3}MC state and the ^{3}MLCT state. This gives rise to the stronger and longer emission of **1a**−**5a**.

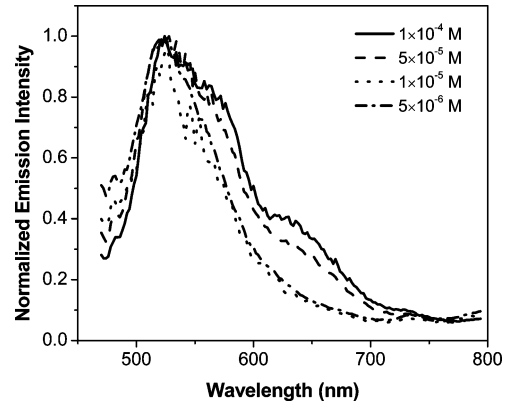

Figure 6. Normalized concentration-dependent emission spectra of **4a** in BuCN glassy solutions at 77 K. The excitation wavelength was 412 nm.

The emission energy and the emission lifetime remain the same for **1a**−**5a** at a concentration range of 5×10^{-6} mol/L to 1×10^{-4} mol/L, and the emission intensity keeps increasing with increased concentration (see Supporting Information Figure S4). This implies that no ground-state aggregation or self-quenching occurs in this concentration range at room temperature.

Similar to the UV−vis absorption, the emission energy and quantum yield of **1a**−**5a** exhibit solvent dependence. Less-polar, noncoordinating solvents, such as CH_2Cl_2, cause a bathochromic shift of the emission band and a higher emission quantum yield. For example, the emission energy of **3a** increases from 625 nm (910 ns) in CH_2Cl_2 to 622 nm (290 ns) in acetone and 619 nm (370 ns) in CH_3CN with increased solvent polarity, which is attributed to the charge-transfer nature of the emitting state. The quantum yield of **4a** is 1.25% in CH_2Cl_2, 0.34% in acetone, and 0.32% in CH_3CN. The reduced emission lifetime and emission quantum yield in CH_3CN should arise from the solvent-quenching effect of CH_3CN.

Complexes **1a**−**5a**, **1b**, **3b**, **4b**, and **5b** exhibit luminescence in a butyronitrile glassy matrix at 77 K. As shown in Figure 5 and tabulated in Table 1, the emission bands shift to higher energies due to the rigidochromic effect[20] and exhibit vibronic structures compared to the emission at room temperature. The emission energy, decay lifetime, and shape of the emission band are similar to those of 4-tolylterpyridyl platinum phenylacetylide and the chloride analogue reported in the literature.[1g–i] In addition, the thermally induced Stokes shift is calculated to be $\Delta E \approx 1360$ cm^{-1} for **1a**, which is a characteristic of a charge-transfer state. Therefore, the emission at 77 K is tentatively assigned to the ^{3}MLCT state as well. The lowest-energy band above 600 nm for **1a**−**5a** and above 580 nm for **1b**, **3b**, **4b**, and **5b** possesses a much shorter lifetime and exhibits a concentration dependence. As exemplified in Figure 6 for **4a**, with increased concentration, the low-energy band at 628 nm increases. However, the excitation spectra monitored at the 570 nm and the 628 nm

(20) (a) Juris, A.; Balzani, V.; Barigelletti, F.; Campagna, S.; Belser, P.; Von Zelewsky, A. *Coord. Chem. Rev.* **1988**, *84*, 85. (b) Cummings, S. D.; Eisenberg, R. *J. Am. Chem. Soc.* **1996**, *118*, 1949. (c) Polo, A. S.; Itokazu, M. K.; Frin, K. M.; Patrocinio, A. O. d. T.; Iha, N. Y. M. *Coord. Chem. Rev.* **2006**, *250*, 1669. (d) Lai, S.-W.; Chan, M. C. W.; Cheung, K.-K.; Che, C.-M. *Inorg. Chem.* **1999**, *38*, 4262.

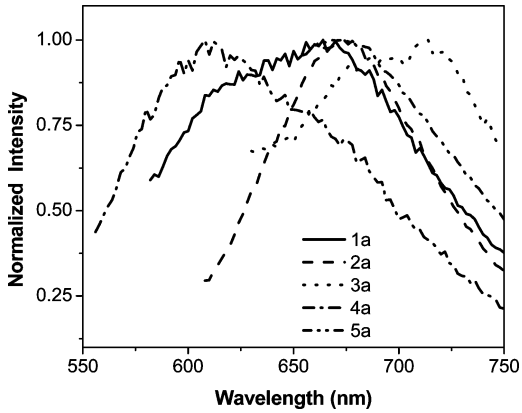

Figure 7. Normalized solid-state emission of **1a**−**5a**. The excitation wavelength was 460 nm.

emission bands are quite similar (see Supporting Information Figure S5), indicating that this low-energy band likely arises from the excimeric emission at higher concentrations. A similar phenomenon has been observed for the other complexes and has been reported by Che and co-workers for platinum(II) 2,6-diphenylpyridine complexes due to the formation of a $^3\pi,\pi^*$ excimer at 77 K.[21]

Solid-state emissions of **1a**−**5a** have also been investigated. As displayed in Figure 7 and compiled in Table 1, all five samples exhibit a broad, structureless emission. Except for **4a**, which exhibits slightly increased emission energy versus that in CH_3CN solution, the emission energies of the other four complexes all decrease in comparison to those in CH_3CN solutions. In view of the similar energy of the solid state emission to those observed in the dinuclear and trinuclear platinum complexes that originate from the triplet metal−metal-to-ligand charge transfer excited state (^{3}MMLCT),[22] the solid-state emission could be assigned to the ^{3}MMLCT state due to intermolecular interaction, which is common for planar platinum(II) terpyridyl complexes in the solid phase. Hannan and co-workers[23] reported that Br−Br interaction existed in the triazine metal complexes, which linked neighbor molecules to form one-dimensional structures. This could also be the case for **4a**, which possesses the chlorine substituent. To fully understand this phenomenon, crystal structure of **4a** needs to be obtained and investigated in the near future.

Triplet Transient Difference Absorption (TA). To figure out the characteristics of the triplet excited-state absorption of **1a**−**5a** and understand the effect of the 4′-pyrimidyl substitution, the time-resolved triplet transient difference absorption spectra of **1a**−**5a** in CH_3CN have been investigated. As shown in Figure 8B, the shape of the transient absorption spectra for all complexes is quite similar, exhibiting a bleaching band from 420 to 500 nm and a broad, moderately intense absorption band between 500 and 800 nm. The positions of the bleaching bands are consistent with the ^{1}MLCT/^{1}LLCT bands in their UV−vis spectra, and the lifetimes of the transients are in line with the lifetimes of the emitting ^{3}MLCT state. Therefore, the transient absorption is tentatively assigned to the ^{3}MLCT state. With reference to our previous work on 4′-tolylterpyridyl platinum(II) phenylacetylide complexes[1i] and other reported work on platinum terpyridyl complexes[3] and ruthenium terpyridyl complexes,[24] the transients that give rise to the observed spectra are presumably attributed to the terpyridyl anion radicals. The transient absorption band maximum of **5a** with a stronger electron-withdrawing −CN substituent appears at a much lower energy (785 nm) in comparison to that of the complex with the electron-donating substituent (**2a**, 720 nm) in CH_3CN.

Using the singlet depletion method,[13] the T_1-T_n absorption coefficients of **1a**−**5a** have been determined. As listed in Table 2, the $\varepsilon_{T_1-T_n}$ values for **1a**, **2a**, **4a**, and **5a** are quite similar, while the $\varepsilon_{T_1-T_n}$ value for **3a** is approximately three times as large as those for **1a**, **2a**, **4a**, and **5a**. This feature should be related to the presence of the phenyl substituent on the pyrimidyl ring, which could enhance the oscillator strength of the transient absorption. Nevertheless, the $\varepsilon_{T_1}-T_n$ values for these complexes are much higher than that observed in a platinum 4-tolylterpyridyl pentynyl complex ($\varepsilon_{T_1-T_n}$ = 26 650 $M^{-1}\cdot cm^{-1}$ at 690 nm),[25] reflecting the significance of coplanarity with the pyrimidyl substituent. The quantum yield of the triplet excited-state formation for **1a**−**5a** in CH_3CN varies from 0.19 to 0.66, which is significantly higher than that of the 4-tolylterpyridyl pentynyl complex ($\Phi_T = 0.16$).[25]

Singlet Oxygen Generation Efficiency. Singlet oxygen can be generated by an energy transfer from the triplet excited state of the photosensitizer to the ground state of oxygen. Recently, several platinum(II) terdentate complexes have been demonstrated to be efficient photosensitizers for the oxidation of olefins and oximes *via* singlet oxygen.[5] Considering the reasonably high triplet excited-state quantum yield of **1a**−**5a** and similar structure features to the reported platinum complexes that generate singlet oxygen, it is expected that **1a**−**5a** could also generate singlet oxygen. To demonstrate this, the singlet oxygen generation quantum yields (Φ_Δ) from **1a**−**5a** have been measured using the method described in the Experimental Section and in the Supporting Information, and the results are listed in Table 2. These values are much higher than that measured for the platinum 4-tolylterpyridyl pentynyl complex ($\Phi_\Delta = 0.019$), which is probably related to the reduced ^{3}MLCT energy as evident by the red-shifted emission spectra at ca. 610−640 nm for **1a**−**5a** with respect to $\lambda_{em} = 580$ nm for the platinum

(21) Lu, W.; Chan, M. C.; Cheung, K.-K.; Che, C.-M. *Organometallics* **2001**, *20*, 2477.
(22) (a) Lu, W.; Chan, M. C. W.; Zhu, N.; Che, C.-M.; Li, C.; Hui, Z. *J. Am. Chem. Soc.* **2004**, *126*, 7639. (b) Kui, S. C. F.; Sham, I. H. T.; Cheung, C. C. C.; Ma, C. W.; Yan, B. P.; Zhu, N. Y.; Che, C. M.; Fu, W. F. *Chem.—Eur. J.* **2007**, *13*, 417. (c) Kui, S. C. F.; Chui, S. S.-Y.; Che, C.-M.; Zhu, N. *J. Am. Chem. Soc.* **2006**, *128*, 8297. (d) Yam, V. W.-W.; Chan, K. H.-Y.; Wong, K. M.-C.; Chu, B. W.-K. *Angew. Chem., Int. Ed.* **2006**, *45*, 6169. (e) Sun, W.; Zhu, H.; Barron, P. M. *Chem. Mater.* **2006**, *18*, 2602. (f) Shao, P.; Sun, W. *Inorg. Chem.* **2007**, *46*, 8603.
(23) Medlycott, E. A.; Udachin, K. A.; Hanan, G. S. *Dalton. Trans.* **2007**, 430.
(24) Co1lin, J.-P.; Guillerez, S.; Sauvage, J.-P.; Barigelletti, F.; De Cola, L.; Flamigni, L.; Balzani, V. *Inorg. Chem.* **1991**, *30*, 4230.
(25) Pritchett, T. M.; Sun, W.; Fuo, F.; Zhang, B.; Ferry, M. J.; Rogers-Haley, J. E.; Shensky, W.; Mott, A. G. *Opt. Lett.* **2008**, *33* (10), 1053.

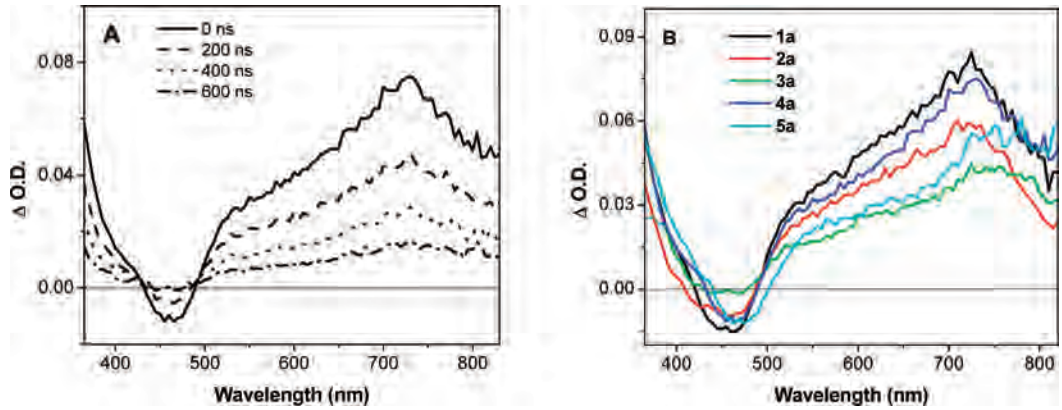

Figure 8. (A) Time-resolved triplet transient difference absorption spectra of **4a** in CH_3CN solution at room temperature. (B) Triplet transient difference absorption spectra of **1a**−**5a** in CH_3CN solution at room temperature at zero time delay. The excitation wavelength was 355 nm.

Table 2. Triplet Excited-State Characteristics of **1a**−**5a** in CH_2Cl_2 and CH_3CN Solutions

	$\lambda_{T1\text{-}Tn}$/nm (τ/ns)[a]				
complex	CH_2Cl_2	CH_3CN	$\varepsilon_{T_1-T_n}$[b]/$M^{-1}\cdot cm^{-1}$	ϕ_T[c]	ϕ_Δ[d]
1a	725(1130)	725(420)	42390	0.65	0.40
2a	725(1560)	720(660)	40710	0.53	0.38
3a	755(910)	755(130)	115090	0.19	0.24
4a	725(920)	730(340)	39030	0.64	0.46
5a	775(330)	785(130)	36600	0.66	0.38

[a] The triplet transient difference absorption band maxima and triplet excited-state lifetimes. [b] The molar extinction coefficients of the triplet excited-state absorption at the band maximum in CH_3CN. [c] Quantum yields of the triplet excited-state formation in CH_3CN. [d] Quantum yields of singlet oxygen generation in CH_3CN.

4-tolylterpyridyl pentynyl complex.[1h] The reduction of the ^{3}MLCT energy could favor the energy transfer from the ^{3}MLCT state to the ground-state oxygen, thus increasing the singlet oxygen generation efficiency. On the other hand, the increased singlet oxygen generation efficiency for **1a**−**5a** could also be attributed to their much longer triplet excited-state lifetimes (130−660 ns) in comparison to that of the platinum 4-tolylterpyridyl pentynyl complex ($\tau_T = 62$ ns).[25]

Nonlinear Transmission. As discussed in the transient absorption section, **1a**−**5a** exhibit a broad triplet excited-state absorption from 500 to 820 nm and possess relatively high triplet excited-state quantum yields (except **3a**) and long lifetimes. Therefore, it is expected that these complexes would exhibit reverse saturable absorption and consequently nonlinear transmission with increased laser fluence in this spectral region. As shown in Figure 9, at a linear transmittance of 75% in a 2 mm cell at 532 nm, the transmission of all five complexes decreases with increased incident fluence, which is the typical phenomenon of nonlinear transmission, and it likely arises from the reverse saturable absorption due to the stronger triplet excited-state absorption versus that of the ground state at 532 nm. At the same linear transmission of 75%, **2a** exhibits the strongest nonlinear transmission, with the transmittance dropping to ~45% at an incident fluence of 1.5 J/cm^2. Complexes **1a** and **4a** exhibit a similar nonlinear transmission to that of **2a**, while the nonlinear transmission of **3a** and **5a** is obviously weaker. Overall, the nonlinear transmissions of **1a**−**5a** are much weaker than that of the 4-tolylterpyridyl platinum phenylacetylide complex reported by our group previously.[1i]

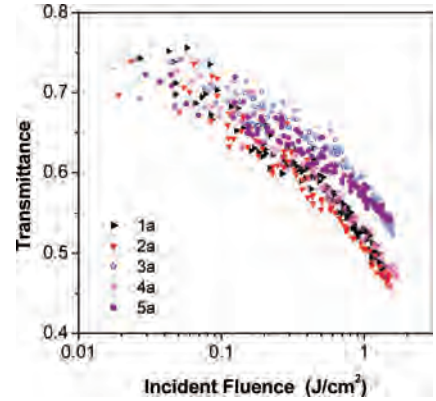

Figure 9. Nonlinear transmission of **1a**−**5a** in CH_3CN solution in a 2 mm cell. The linear transmission was adjusted to 75%.

Table 3. Ground-State and Triplet Excited-State Absorption Cross-Sections of **1a**−**5a** in CH_3CN at 532 nm

complex	σ_0[a]/ cm^2	σ_T[b]/cm^2	σ_T/σ_0	$\sigma_T\Phi_T/\sigma_0$
1a	1.30×10^{-18}	6.01×10^{-17}	46.2	30.0
2a	1.07×10^{-18}	6.09×10^{-17}	56.9	30.2
3a	1.53×10^{-18}	1.60×10^{-16}	104.5	19.9
4a	1.69×10^{-18}	5.72×10^{-17}	33.8	21.6
5a	4.60×10^{-18}	4.54×10^{-17}	9.9	6.5

[a] The ground-state absorption cross-section. [b] The triplet excited-state absorption cross-section.

To explain these differences, the parameters that are directly related to the nonlinear transmission, that is, the ratio of the excited-state absorption cross-section to that of the ground state (σ_T/σ_0), and the triplet excited-state quantum yield (Φ_T), need to be closely examined. A larger ratio of $\sigma_T\Phi_T/\sigma_0$ generally leads to a stronger nonlinear transmission. To figure out this ratio, it is first necessary to estimate the triplet excited-state absorption coefficient (ε_T) at 532 nm using the method described in the Supporting Information. The ε_T's at 532 nm are estimated to be 15 700 $M^{-1}cm^{-1}$ for **1a**, 15 910 $M^{-1}cm^{-1}$ for **2a**, 41 880 $M^{-1}cm^{-1}$ for **3a**, 14 940 $M^{-1}cm^{-1}$ for **4a**, and 11 860 $M^{-1}cm^{-1}$ for **5a**. These ε_T's can then be converted to the triplet excited-state absorption cross-section (σ_T) using the conversion equation $\sigma = 2303\varepsilon/N_A$, where N_A is the Avogadro constant. The results are listed in Table 3. It is important to note that the key parameter that determines the nonlinear transmission is the ratio of $\sigma_T\Phi_T/\sigma_0$, not just σ_T. σ_0 can be calculated from the molar extinction coefficient of UV−vis absorption at 532 nm,

which is also tabulated in Table 3. Comparing the σ_0's of **1a**−**5a** at 532 nm to that of the 4-tolylterpyridyl platinum phenylacetylide complex (2.43×10^{-19}),[1i] they are 4.4−18.9 times larger. This would cause a decreased ratio of $\sigma_T\Phi_T/\sigma_0$ in the case of a similar σ_T and Φ_T, and therefore a weaker nonlinear transmission. Among **1a**−**5a**, the $\sigma_T\Phi_T/\sigma_0$ values for **1a**, **2a**, and **4a** are larger than those for **3a** and **5a**, which are consistent with the trend observed from the nonlinear transmission measurement. Other factors that might contribute to the difference in nonlinear transmission is the triplet excited-state lifetime, which is much longer for **2a**, comparable for **1a** and **4a**, and much shorter for **3a** and **5a**.

Conclusion

4′-(5‴-R-Pyrimidyl)-2,2′;6′,2″-terpyridine platinum(II) phenylacetylide complexes (**1a**−**5a**) exhibit moderately intense ^{1}MLCT/^{1}LLCT absorption in their UV−vis spectra, the energy of which is influenced by the 5‴ substituent. All complexes emit at room temperature, 77 K, and in the solid state, and the emitting state is tentatively assigned to the ^{3}MLCT state. The emission energy at room temperature exhibits a linear correlation with the Hammett σ_p constant of the 5‴ substituent, indicating the electron delocalization ability of the pyrimidyl group. All complexes exhibit a broad, moderately intense triplet excited-state absorption from 500 to 820 nm, which is presumably attributed to the terpyridyl anion radical. Except for **3a**, the other four complexes exhibit relatively high quantum yields of the triplet excited-state formation. This subsequently leads to the formation of singlet oxygen in a much higher quantum yield in comparison to the 4-tolyterpyridyl platinum pentynyl complex. In addition, all complexes exhibit a moderate nonlinear transmission at 532 nm for nanosecond laser pulses, and the difference in their nonlinear transmission behavior arises from the differing ratio of $\sigma_T\Phi_T/\sigma_0$.

Acknowledgment. Acknowledgment is made to the National Science Foundation (CAREER CHE-0449598) and Army Research Laboratory (W911NF-06-2-0032) for support. We are also grateful to North Dakota State EPSCoR (ND EPSCoR Instrumentation Award) for support.

Supporting Information Available: Plots of the lowest-energy UV−vis absorption band energy and the emission band energy vs Hammett σ_p constant of the 5-pyrimidinyl substituent; concentration-dependent emission spectra of **1a** at room temperature; concentration-dependent excitation spectra of **2a** at room temperature; excitation spectra of **2a** monitored at different wavelengths at 77 K; and time-resolved triplet transient difference absorption spectra of **1a**, **2a**, **3a**, and **5a** in CH_3CN. This material is available free of charge via the Internet at http://pubs.acs.org.

IC800358W